EVALUATION OF A FULLY DIGITAL, IN-HOUSE VIRTUAL SURGICAL PLANNING WORKFLOW FOR BIMAXILLARY ORTHOGNATHIC SURGERY

by

DAVID GAGNIER

Submitted in partial fulfilment of the requirements
Of the degree of Master of Science

at

Dalhousie University
Halifax, Nova Scotia
March 2024

Dedication

I would like to dedicate this work to my amazing wife, Eunnie, and our son, Hugh. Thank you for being a constant source of inspiration and joy.

Table of Contents

List of Tables

List of Figures

Abstract

The advantages of virtual surgical planning (VSP) for orthognathic surgery are clear. Previous studies have evaluated in-house VSP, however, few fully digital, in-house protocols for orthognathic surgery have been studied. The authors developed a fully digital, in-house VSP workflow for orthognathic surgery and assessed its accuracy in a prospective cohort of 52 patients who underwent bimaxillary orthognathic surgery. The predictor variables were VSP using the established protocol and the surgical sequence (mandible-first or maxilla-first). The outcome variables were the mean 3D distance error, as well as mean error and mean absolute error in the left-right (x axis), superior-inferior (y axis), and anterior-posterior (z axis) dimensions. In general, the largest contributor to mean 3D distance error was deficient movement in the anterior-posterior direction (z axis). This finding was felt to be clinically valuable for treatment planning purposes when using a fully digital, in-house VSP workflow.

List of Abbreviations

ANOVA	Analysis of variance
CAD	Computer-aided design
CAM	Computer-aided manufacturing
CASS	Computer-aided surgical simulation
CBCT	Cone-beam computed tomography
CT	Computed tomography
DICOM	Digital imaging and communications in medicine
IOS	Intraoral scan
ICC	Intraclass correlation coefficient
NHP	Natural head position
OMFS	Oral and maxillofacial surgery
OSA	Obstructive sleep apnea
PSI	Patient-specific implant
R-VBR	Regional voxel-based registration
SLA	Stereolithography
STL	Standard tessellation language
VSP	Virtual surgical planning

Acknowledgments

I would like to acknowledge my thesis supervisor Dr. Curtis Gregoire for his expertise and guidance throughout this process. I would also like to thank my internal and external reviewers, Drs. James Brady and Sanjay Anand for their thoughtful contributions to this manuscript.

Additionally, I would like to thank my co-residents for their patience and remarkable willingness to learn. Specifically, I would also like to thank my good friend and colleague Dr. Chad Sampson for his important contribution to this thesis topic.

My sincere thanks go to my summer research students Dr. Andra Sterea and Dr. Taylor Chaput for their incredible work ethic and commitment to this project.

I would also like to thank Kelly Davis and the other support staff in the department for their tireless efforts in patient recruitment and retainment.

I would also like to thank Dr. Hong Gu and Yurunyun Yang for their contributions to statistical analysis and expert input into discussions around data interpretation.

Lastly, I would like to thank the Canadian Association of Oral and Maxillofacial Surgeons for their funding contributions.

Chapter 1: Introduction and Review of the Literature

1.1 Orthognathic Surgery and Planning Techniques

Orthognathic surgery has been a mainstay treatment for the dentofacial deformity for decades. Surgical techniques have evolved to improve the predictability of the procedure, decrease the frequency of complications, and improve patient outcomes. More recently, the process of surgical planning has made significant improvements with advances in imaging and software. Orthognathic surgery is a highly complex procedure, and a meticulous surgical plan is critical to the success of the operation.

Traditionally, "model surgery" has been a widely used method for diagnosis, planning, and simulation in orthognathic surgery. This technique involves the acquisition of dental impressions, a bite registration, and a facebow transfer of the maxillary position in relation to the glenoid fossae. Dental models are mounted on a semi-adjustable articulator in centric relation, cut, and manipulated to simulate the desired surgical outcome. This is done in conjunction with lateral cephalometric radiographs and patient photos. Finally, occlusal splints are fabricated by hand to facilitate accurate intraoperative positioning of the jaws according to the plan.

Despite its widespread use, several limitations exist with traditional model surgery. First, the process of obtaining and preparing preoperative records is laborious and involves multiple steps. This workflow relies heavily on the accuracy of a technician, allowing for the introduction and magnification of error at each stage of the process. Second, stone models do not replicate bony structures beyond the alveolus and palate. For this reason, osteotomies in stone models are inherently not accurate. Finally, the use of plain-film radiographs for surgical planning purposes is limited due to their two-dimensional nature.

More recently, virtual surgical planning (VSP) has modernised the process of surgical planning and simulation for orthognathic surgery. With the use of three-

dimensional imaging, digital occlusal records, and specialized planning software, clinicians can analyse and manipulate the maxillomandibular complex virtually in three-dimensions. VSP has also enabled the use of computer-aided design and manufacturing (CAD/CAM) of occlusal splints, patient-specific guides, and patient-specific implants (PSIs) to more accurately reproduce the virtual plan in the operating room.

1.2 Virtual Surgical Planning for Orthognathic Surgery

Among the first to use VSP for orthognathic surgery were Gateno and Xia in 2007.[1] They described a method of computer-aided surgical simulation (CASS) that involved using a bite jig and a series of fiducial markers to combine a CT skull model with digital dental models. The resulting composite skull model displayed an accurate rendition of both the bony structures and teeth which was not previously possible with a CT scan alone. Next, they performed simulated surgeries on a computer and created surgical splints and guides with CAD/CAM to help reproduce the virtual plan in the operating room. This technique introduced several advantages including the ability to treat complex asymmetries in fewer procedures as well as improved surgical accuracy.[1]

In 2009, Swennen et al improved the VSP workflow for orthognathic surgery with a "triple scan" technique to create a composite skull model. This involved voxel-based registration of the skull and a dental impression, removing the need for a bite jig with fiducial markers.[2] In 2016, De Waard et al showed that a digital intra-oral scan could be fused with a CBCT to create a more detailed representation of the dentition, eliminating the need for conventional impressions altogether.[3,4] The use of digital intra-oral scans as an alternative to conventional plaster casts has been further supported by recent literature.[5]

The advantages of VSP for orthognathic surgery have been well established in the literature. Several studies comparing the accuracy of VSP with CAD/CAM splints to conventional model surgery have shown that VSP is comparable or more accurate.[6–9] The accuracy of VSP has been especially noted in cases involving a facial asymmetry.[8]

Additionally, the operative time tends to be significantly less with VSP than with conventional planning due to the ability to use patent-specific surgical guides.[10]

1.2.1 Implementing the Virtual Plan

Currently, there are several ways to implement CASS for the planning and execution of orthognathic surgery with patient-specific guides. The most common and least resource intensive patient-specific guides are occlusal splints. In a mandible-first surgical sequence, an "intermediate splint" is used to position the osteotomized mandible based on the native position of the maxilla. A "final splint" is then used to position maxilla based on the new position of the mandible. In a maxilla-first sequence, the intermediate splint is used to position the maxilla and the final splint is used to position the mandible. Other authors have proposed using a combination of occlusal splints as well as cutting and positioning templates to more accurately reproduce the virtual plan.[11] A variation of this technique involves 3D printing the simulated postoperative skull and prebending plates that are later sterilized and used to position the maxilla during surgery. A more contemporary protocol involves the use of patient-specific implants. In this technique, custom drill/cutting guides, and a single custom PSI (plate) are used for maxillary repositioning without the need for an intermediate splint.[12–17] Recent studies have suggested that a PSI is more accurate in reproducing the virtual plan than occlusal splints alone for orthognathic surgery.[12,17,18] Despite the accuracy, PSI is significantly more expensive than other techniques. Ultimately, the surgeon must decide which technique is most appropriate given the clinical scenario.

1.2.2 In-House VSP

Many of the previously described VSP protocols rely on a third-party company to facilitate the planning process. During a web conference, the virtual plan is executed by a biomedical engineer and finalized by the surgeon. The company then manufactures the necessary surgical splints and guides which are mailed to the surgeon prior to the operation. The main limitations of this protocol are the additional time required to

manufacture and transport the surgical guides, as well as the increased cost to the surgeon and/or patient.[19]

To circumvent the need for a third-party, "in-house" VSP protocols for surgical planning have been suggested. In 2015, Mendez et al used an in-house protocol to manufacture customized skull models for craniofacial reconstruction that was more cost effective and less time consuming.[19] In 2020, Sharkh et al described an in-house VSP technique for microvascular reconstruction using free software.[20]

In-house VSP techniques specific to orthognathic surgery have also been described. In 2021, Mascarenhas described an efficient in-house 3D printing technique for single-jaw orthognathic surgery that took less than 5 minutes to design a surgical splint.[21] However, this technique involved mounting stone models on an articulator, setting the occlusion by hand, and scanning the final occlusion with an intraoral scanner (steps which were not included in the total time).

In 2020, De Riu et all described a new protocol for in-house management of computer assisted simulation for bimaxillary orthognathic surgery.[22] This protocol involved pouring stone models, importing a CBCT of the models into an open-source software for processing, then using a second imaging software for surgical simulation.

Many authors have described similar in-house VSP techniques, however, few fully digital, in-house protocols have been discussed for bimaxillary orthognathic surgery.

Chapter 2: Purpose Statement

The purpose of this study was to establish a fully digital, in-house VSP workflow for orthognathic surgery and to evaluate its accuracy. The investigators hypothesized that this workflow could provide a range of error that meets criteria for clinical acceptability commonly used in the literature.[9] The specific aim of this study was to measure the 3D distance error, as well as the mean error and mean absolute error in the left-right, superior-inferior, and anterior-posterior dimensions, for a series of landmarks between the virtual surgical plan and the actual surgical outcome.

Chapter 3: Materials and Methods

3.1 Study Design

This prospective cohort recruited patients undergoing orthognathic surgery for the correction of a dentofacial deformity between September 2020 and November 2022. The study was reviewed and approved by the institutional ethics committee, the Nova Scotia Health Authority Research Ethics Board.

3.2 Subject Selection

All patients who were scheduled to undergo orthognathic surgery at the Department of Oral and Maxillofacial Surgery at the Victoria General Hospital in Halifax, NS, Canada (Dalhousie University) were invited to participate in the study, providing they met the following criteria.

Inclusion criteria:

i. Patients requiring both maxillary and mandibular surgery, with or without genioplasty
ii. Patients undergoing concurrent orthodontic treatment with conventional fixed appliances
iii. Patients undergoing concurrent orthodontic treatment with clear aligner appliances

Exclusion criteria:

i. Patients who have previously undergone orthognathic surgery
ii. Patients with a cleft lip and/or palate
iii. Patients with a craniofacial syndrome

Patients were invited to participate in the study at the time of their preadmission appointment. All potential benefits and harms related to the study were reviewed and a formal informed consent agreement was signed.

3.3 Variables

The primary predictor variable was VSP using the fully digital, in-house protocol. The secondary predictor variable was the surgical sequence (mandible-first or maxilla-first). The primary outcome variable was the mean 3D (Euclidean) distance error as well as the mean error and mean absolute error in the left-right (x axis), superior-inferior (y axis), and anterior-posterior (z axis) dimensions between the actual surgical movement and the virtual surgical plan for each landmark. Covariates included age and sex. The mean 3D distance error was calculated as follows:

$$Mean\ 3D\ Distance\ Error = \frac{1}{n}\sum_{k=1}^{n}\sqrt{(x_{operation,k} - x_{VSP,k})^2 + (y_{operation,k} - y_{VSP,k})^2 + (z_{operation,k} - z_{VSP,k})^2} \quad (1)$$

3.4 Data Collection Methods

3.4.1 Preoperative Planning Protocol

The typical sequence of preoperative appointments for orthognathic surgery consisted of an initial consultation followed by a preadmission appointment. At the initial consultation, a thorough medical history and head and neck examination was performed with a focus on the maxillofacial structures. Preliminary investigations were obtained as required to develop a diagnosis and tentative surgical treatment plan. An approximate surgery date was then selected in collaboration with the referring orthodontist based on the progress of the presurgical orthodontic setup.

Within one to two weeks of the surgery date, patients then presented for a preadmission appointment. A detailed examination of the maxillofacial complex was repeated and preoperative records were obtained. At this time, patients who met the inclusion and exclusion criteria were invited to participate in the study (see Section 3.2

Subject Selection). For the purposes of the study, these preoperative records included a panoramic and lateral cephalometric radiograph, a CBCT image (i-CAT FLX V17; DEXIS™ dental imaging solutions, Quakertown, PA, USA), and a digital impression using an intraoral scanner (Primescan; Dentsply Sirona, Charlotte, NC, USA). CBCTs were obtained using a preestablished protocol that included a 0.3 mm voxel size and 23 x 17 cm field of view image (DAP: 877.6 mGy-cm^2) taken with the patient in maximum intercuspation in the natural head position. The natural head position was achieved by asking the patient to sit upright, looking straight ahead toward a mirror at eye level on the opposing wall.[23]

The CBCT (DICOM dataset) and intraoral scan (STL file) were then imported into a planning program (Dolphin Imaging v11.95 and v12 beta; Patterson Dental, Saint Paul, MN, USA). First, the digital model was superimposed onto the 3D volume using a combination of the auto superimpose function and manual manipulation. The final position of the superimposition was then verified in three planes using the slice views. Next, the orthognathic surgery planning module was used to setup and plan the surgery in a stepwise fashion. Steps 1 through 5 involved cropping and clean-up of the STL converted volume, followed by osteotomizing the maxilla and mandible. These steps were carried out by a member of the surgical resident team. The final occlusion was set virtually and the desired surgical movements made based on a Delaire analysis of the lateral cephalometric radiograph in Steps 6 and 7.[24] These steps were carried out by the operating resident and reviewed by the staff surgeon. The intermediate and final occlusal splints where then designed in Step 8 of the module by the first-year surgical resident.

The finalized splints (STL files) were then optimized for printing with a print preparation program (Preform; Formlabs, Somerville, MA, USA) and printed with an SLA 3D printer (Form 3B; Formlabs, Somerville, MA, USA). Post-print processing included washing (Form Wash; Formlabs, Somerville, MA, USA) and curing (Form Cure; Formlabs, Somerville, MA, USA) of the parts. Finishing and polishing of the parts was carried out by the first-year surgical resident.

3.4.2 Surgical Protocol

All patients underwent LeFort I osteotomies (single-piece or multi-piece) and bilateral sagittal split osteotomies. Some patients also underwent a genioplasty if indicated. The surgeries were carried out in the operating room (Victoria General Hospital, Halifax, NS, Canada) under general anesthesia by one of the five staff surgeons at the Department of OMFS at Dalhousie and a resident. The prefabricated intermediate splint was used to stabilize the intermediate position for plating. Both mandible-first and maxilla-first approaches were used, depending on the virtual surgical plan. The final splint was then used to stabilize the final occlusion for plating. LeFort I osteotomies were fixated with 2.0 mm KLS Martin titanium plates at the level of the nasal aperture and either 2.0 mm KLS Martin plates or wire osteosynthesis at the zygomatic buttresses. Bilateral sagittal split osteotomies were fixated with crescent shaped 2.0 mm KLS Martin titanium plates. Patients were then placed into maxillomandibular fixation with the final splint in place using orthodontic elastics for a period of two to four weeks postoperatively.

3.4.3 Follow-up Protocol

Patients were generally seen for follow-up at two, four, and six weeks postoperatively. The occlusal splint was removed at either two or four weeks and a postoperative CBCT was obtained at the same appointment. The same protocol for obtaining the preoperative CBCT was used (see Section 3.4.1 Preoperative Planning Protocol). The postoperative CBCT DICOM data was then imported once again into Dolphin Imaging software for analysis. The complete workflow for data collection and analysis is illustrated in Figure 1.

The postoperative analysis involved two broad steps: registration of the postoperative volume and landmarking of both the preoperative and postoperative volumes. First, registration of the postoperative volume to the preoperative volume was accomplished using a validated, semiautomated, voxel-based superimposition based on the cranial base [25,26] (Figure 2). Next, a series of 23 predefined cephalometric landmarks

(Figure 3) were labelled using a standardized protocol (see Appendix 1: Standardized Landmarking Protocol) on the preoperative virtual plan, as well as both the preoperative and postoperative volumes by two of three independent observers (AS, TC, and DG). The first fifteen cases were landmarked twice by each observer (AS and DG) on separate occasions for intra-observer reliability calculation purposes.

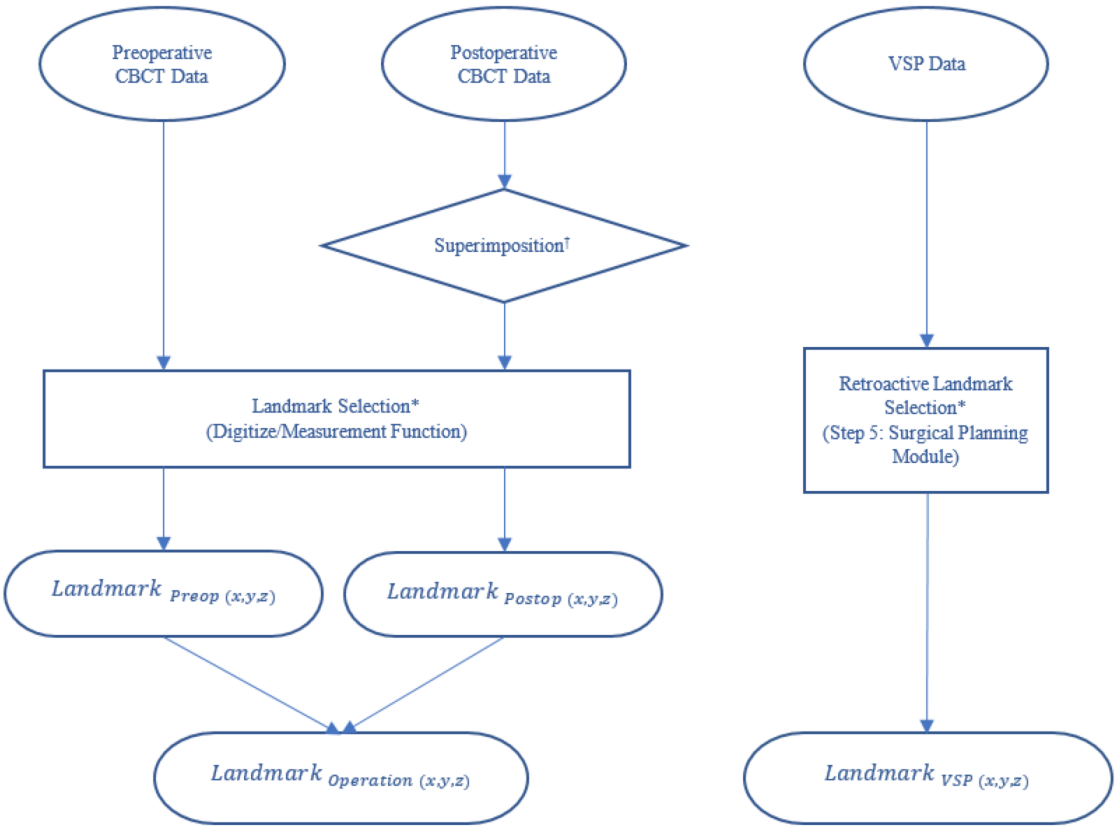

Figure 1. Data collection and analysis workflow.

† Semiautomated, voxel-based superimposition of the postoperative volume onto the preoperative volume

* 23 cephalometric landmarks using a standardized protocol

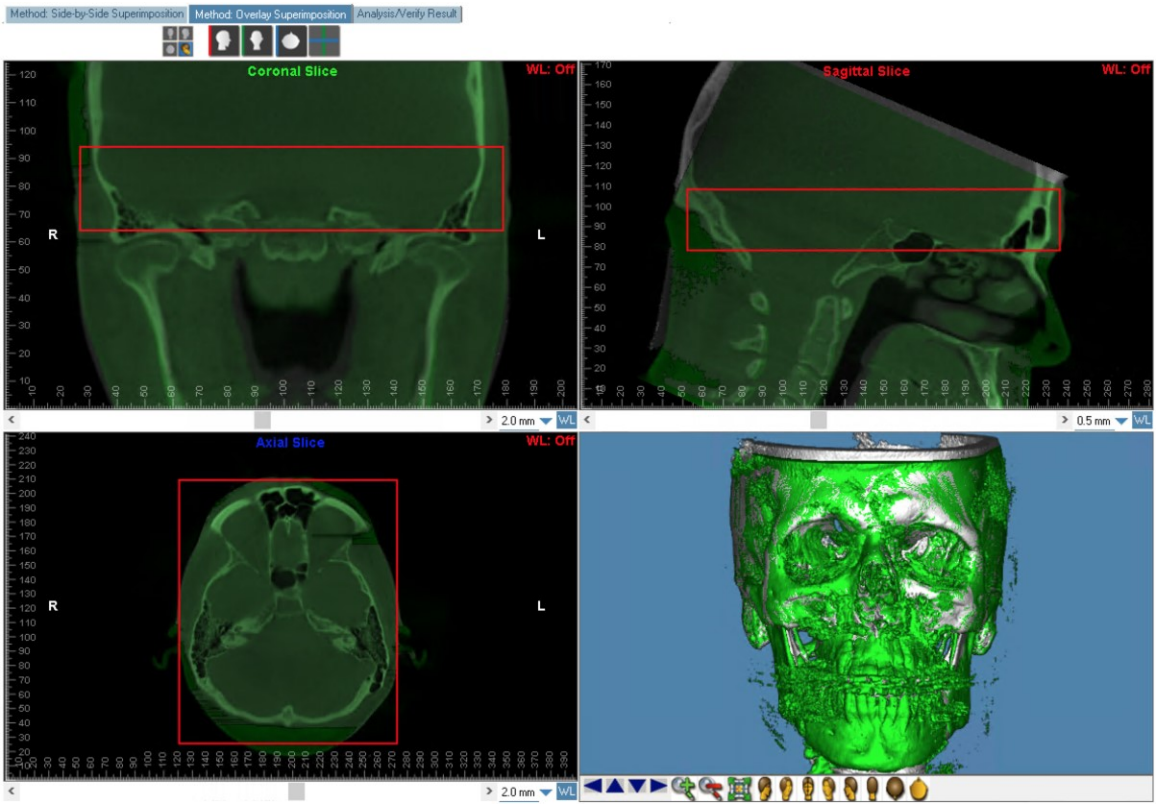

Figure 2. Voxel-based superimposition of the postoperative volume onto the preoperative volume.

3.4.4 Evaluation of the Virtual Surgical Plan

The preoperative virtual plan was landmarked in a retroactive fashion in Step 5 of the orthognathic surgery planning module by one of the three independent observers to ensure it was completed according to the standardized landmarking protocol. These landmarks were then automatically carried forward to the previously established virtual surgical plan in Step 6 of the planning module. The landmark offsets (planned surgical movements) in three dimensions for each of the landmarks were then exported from the Landmark Offset and Measurement Tables in the form of a linear distance in millimetres.

3.4.5 Evaluation of the Postoperative Outcome

The preoperative and postoperative volumes were landmarked using the same standardized protocol. The position of the landmarks in three dimensions were then exported from both volumes in the form of x, y, and z coordinates in millimeters. The difference between the postoperative and preoperative landmarks were calculated, giving the actual surgical movements in the form of a linear distance in millimetres. For patients who underwent a genioplasty, landmarks B-point, gnathic, menton, and pogonion were excluded as these were obscured by hardware artifact.

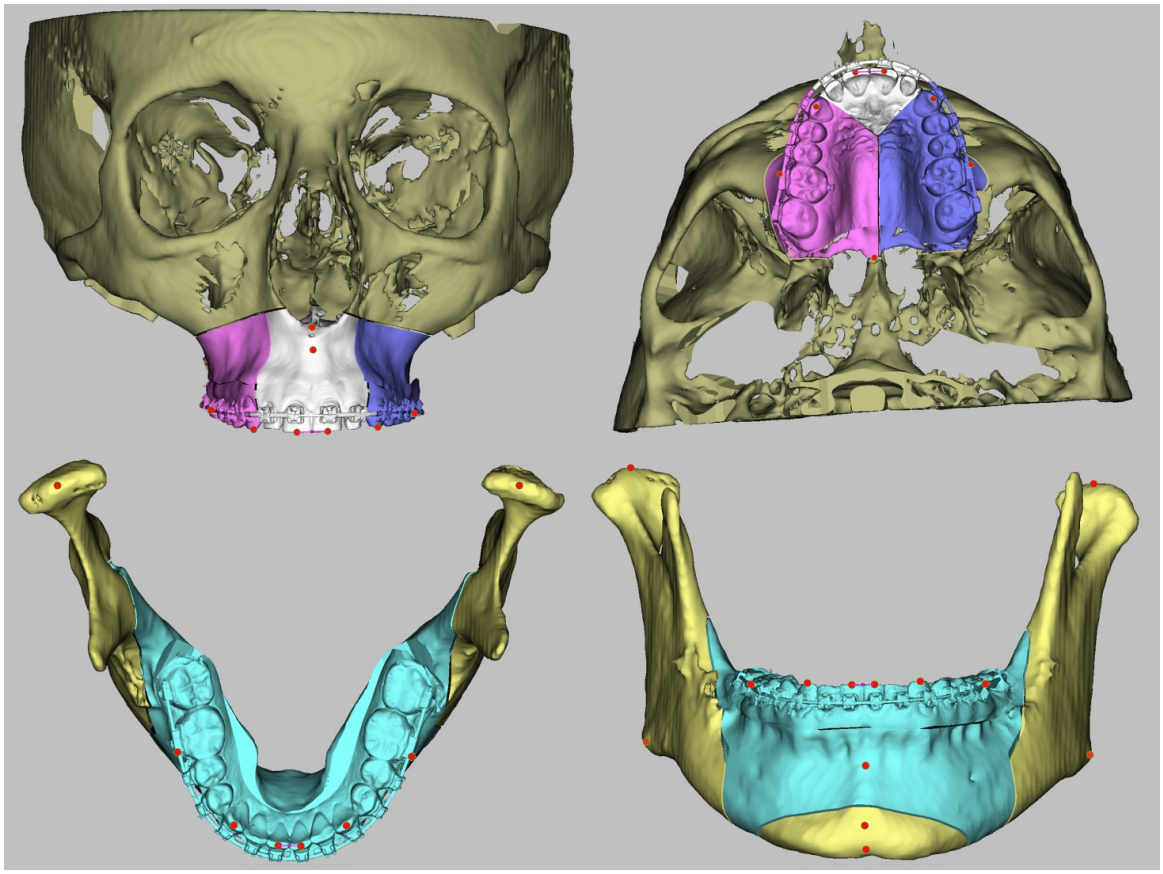

Figure 3. The 23 landmarks used to evaluate the postoperative outcome.

3.5 Data Analyses

All statistical analyses were carried out by Dr. Hong Gu and Yurunyun Yang in the Department of Mathematics and Statistics at Dalhousie University, Halifax, NS. These statistical services were partially funded by a Mitacs research grant.

3.5.1 Sample Size Calculation

A sample size calculation was performed for the mean 3D distance error assuming a standard error of 0.2 mm. The sample size needed for statistical power was calculated for each landmark and a sample size of 50 was adequate for most landmarks, including the maxillary central incisor. The results for the sample size calculation are presented in Appendix 2, Supplemental Table 9.

3.5.2 Inter-Observer and Intra-Observer Reliability

The inter-observer and intra-observer reliability for manual landmark labelling were assessed using the intraclass correlation coefficient (ICC). A two-way mixed consistency model (ICC[3,1]) was selected as multiple observers provided measurements on the same subjects, the raters were considered to be a fixed set of raters, and generalization of the results to other raters was not of interest. An ICC between 0.5 and 0.75 represented moderate reliability, between 0.75 and 0.9 represented good reliability and greater than 0.9 was considered excellent. The mean absolute inter and intra-observer measurement error was also calculated.

3.5.3 Statistical Tests

The primary outcomes were assessed using a Z critical value confidence interval for the mean 3D distance error as well as mean and absolute distance error in the left-right, superior-inferior, and anterior-posterior dimensions across all patients. A 95% confidence interval was used. A *t* critical value confidence interval was used to assess the mean 3D distance error for the mandible-first surgery and maxilla-first surgery groups.

Once again, a 95% confidence interval was used. In keeping with the literature, 2 mm was considered to be the error threshold for clinical acceptability.[9] The effect of surgical sequence on 3D distance error was tested using a two-sample *t*-test as well as analysis of variance (ANOVA).

Chapter 4: Results

4.1 Patient Characteristics

The study group consisted of 52 patients (24 males and 28 females) who underwent bimaxillary orthognathic surgery. The mean age of the study group was 27.7 years old with ages ranging from 15 to 65 years old. Of these patients, 11 underwent segmental Lefort osteotomies and 14 underwent concurrent genioplasty. 43 patients underwent a mandible-first surgical sequence and 9 patients underwent a maxilla-first surgical sequence. Five patients underwent maxillomandibular advancement for obstructive sleep apnea.

4.2 Inter-Observer and Intra-Observer Reliability

The evaluation of inter and intra-rater reliability for landmark labelling is presented in Table 2. The ICC ranged from moderate to excellent and the mean absolute measurement error ranged from 0.37 to 0.52 mm in the left-right dimension, 0.35 to 0.93 mm in the superior-inferior dimension, and 0.43 to 0.69 mm in the anterior-posterior dimension.

Table 1. Patient demographics

Study Variable	Operation Sequence		Total
	Mandible-first	Maxilla-first	
Sex			
Male	20	4	24 (46.2%)
Female	23	5	28 (53.8%)
Total	43	9	52 (100%)
Mean Age (± SD)	27.7 ± 11.3	27.7 ± 16.5	27.7 ± 12.1

Abbreviations: SD, standard deviation

Table 2. Inter and intra-observer reliability for landmark labelling

Dimension	Intra-observer reliability (DG1 & DG2)		Inter- observer reliability (DG1 & AS)		Inter- observer reliability (DG1 & TC)	
	ICC*	Abs. (mm)†	ICC*	Abs. (mm)†	ICC*	Abs. (mm)†
x	0.89	0.37	0.80	0.52	0.83	0.38
y	0.94	0.35	0.93	0.93	0.74	0.57
z	0.93	0.44	0.94	0.67	0.92	0.43

* Intraclass correlation coefficient. ICC values less than 0.5 are indicative of poor reliability, values between 0.5 and 0.75 indicate moderate reliability, values between 0.75 and 0.9 indicate good reliability, and values greater than 0.90 indicate excellent reliability.

† Absolute measurement error mean in millimeters

4.3 Primary Outcomes

4.3.1 Mean 3D Distance Error

The Z critical value confidence interval for the mean 3D distance error for each landmark across all patients is presented in Table 3. The mean 3D distance error was smallest for the left and right condyle landmarks, which were 1.72 mm and 1.68 mm, respectively. The mean 3D distance error for dental landmarks ranged from 2.79 mm at the left mandibular canine to 3.15 mm at the right maxillary molar. For the left and right maxillary central incisors, the mean 3D distance error was 2.86 mm and 2.93 mm, respectively. The mean 3D distance error was largest for the bony landmarks and ranged from 3.23 mm at menton and 4.59 mm at ANS.

4.3.2 Mean Distance Error

The Z critical value confidence interval for the mean distance error for each landmark in the left-right, superior-inferior, and anterior-posterior dimensions across all patients is presented in Table 4 and Table 5 for maxillary and mandibular landmarks, respectively. The mean distance error was negative in the anterior-posterior dimension (z axis) for all landmarks and this result was statistically significant for all landmarks except gnathion (P = 0.07), menton (P = 0.06), and pogonion (P = 0.06). The mean distance error for the left and right maxillary central incisor landmarks in the x, y, and z dimensions are illustrated in Figure 4.

4.3.3 Mean Absolute Distance Error

The Z critical value confidence interval for the mean absolute distance error for each landmark in the left-right, superior-inferior, and anterior-posterior dimensions across all patients is presented in Table 6 and Table 7 for maxillary and mandibular landmarks, respectively. The mean absolute distance error was largest in the anterior-posterior dimension (z axis) for all landmarks except PNS, left condyle, and gonion (left and right). For the maxillary central incisors, the mean absolute distance error was less than 1 mm in

the superior-inferior dimension (y axis) and less than 2 mm in the left-right (x axis) and anterior-posterior dimensions (z axis).

Table 3. Landmark vs mean 3D distance error

Landmark		Mean (mm)†	95% CI‡	
L1	A-point	4.03	[3.55,	4.50]
L2	ANS	4.59	[3.97,	5.20]
L3	PNS	3.39	[3.01,	3.78]
L4	Mx Canine (L)	2.81	[2.42,	3.20]
L5	Mx Canine (R)	2.86	[2.49,	3.24]
L6	Mx Molar (L)§	3.05	[2.63,	3.47]
L7	Mx Molar (R)§	3.15	[2.79,	3.52]
L8	Mx Incisor (L)¥	2.86	[2.49,	3.23]
L9	Mx Incisor (R)¥	2.93	[2.54,	3.33]
L10	B-point	3.24	[2.72,	3.75]
L11	Condyle (L)	1.72	[1.41,	2.04]
L12	Condyle (R)	1.68	[1.39,	1.98]
L13	Gnathion	3.29	[2.76,	3.81]
L14	Gonion (L)	3.64	[3.02,	4.26]
L15	Gonion (R)	4.22	[3.46,	4.98]
L16	Md Canine (L)	2.79	[2.39,	3.19]
L17	Md Canine (R)	3.08	[2.68,	3.49]
L18	Md Molar (L)§	3.05	[2.64,	3.45]
L19	Md Molar (R)§	3.12	[2.70,	3.55]
L20	Md Incisor (L)¥	2.97	[2.60,	3.35]
L21	Md Incisor (R)¥	2.93	[2.55,	3.31]
L22	Menton	3.23	[2.68,	3.77]
L23	Pogonion	3.36	[2.82,	3.89]

Abbreviations: ANS, anterior nasal spine; PNS, posterior nasal spine; Mx, maxillary; Md, mandibular; L, left; R, right; CI, confidence interval.

§ First molar.

¥ Central incisor.

† Mean of the 95% confidence interval expressed in millimeters.

‡ Z critical value confidence interval.

Table 4. Landmark vs mean distance error (maxillary landmarks)

Landmark		Dimension	Mean (mm)†	95% CI‡		P value
L1	A-point	x	-0.63	[-1.02,	-0.24]	<.01
		y	-0.99	[-1.59,	-0.38]	<.01
		z	-2.73	[-3.28,	-2.17]	<.01
L2	ANS	x	-0.65	[-1.05,	-0.24]	<.01
		y	-0.13	[-0.54,	0.28]	.52
		z	-3.92	[-4.60,	-3.23]	<.01
L3	PNS	x	-0.45	[-1.00,	0.11]	.11
		y	1.26	[0.73,	1.78]	<.01
		z	-1.10	[-1.60,	-0.60]	<.01
L4	Mx Canine (L)	x	-0.64	[-1.02,	-0.25]	<.01
		y	0.43	[0.11,	0.76]	.01
		z	-1.77	[-2.26,	-1.29]	<.01
L5	Mx Canine (R)	x	-0.42	[-0.81,	-0.03]	.03
		y	0.53	[0.23,	0.83]	<.01
		z	-1.81	[-2.32,	-1.30]	<.01
L6	Mx Molar (L)§	x	-0.86	[-1.25,	-0.47]	<.01
		y	0.62	[0.28,	0.96]	<.01
		z	-1.86	[-2.40,	-1.32]	<.01
L7	Mx Molar (R)§	x	-0.25	[-0.59,	0.09]	.15
		y	0.75	[0.43,	1.06]	<.01
		z	-2.15	[-2.69,	-1.61]	<.01
L8	Mx Incisor (L)¥	x	-0.45	[-0.87,	-0.04]	.03
		y	0.12	[-0.25,	0.48]	.52
		z	-1.71	[-2.19,	-1.22]	<.01
L9	Mx Incisor (R)¥	x	-0.64	[-1.09,	-0.19]	<.01
		y	0.13	[-0.25,	0.51]	.49
		z	-1.71	[-2.19,	-1.24]	<.01

Abbreviations: ANS, anterior nasal spine; PNS, posterior nasal spine; Mx, maxillary; Md, mandibular; L, left; R, right; CI, confidence interval.

§ First molar.

¥ Central incisor.

† Mean of the 95% confidence interval expressed in millimeters.

‡ Z critical value confidence interval. Null hypothesis was that the mean distance error was 0.

Table 5. Landmark vs mean distance error (mandibular landmarks)

Landmark		Dimension	Mean (mm)†	95% CI‡		P value
L10	B-point	x	-0.52	[-1.01,	-0.04]	.03
		y	1.45	[0.75,	2.15]	<.01
		z	-1.27	[-2.04,	-0.51]	<.01
L11	Condyle (L)	x	0.29	[-0.06,	0.63]	.10
		y	-0.53	[-0.78,	-0.28]	<.01
		z	-0.77	[-1.05,	-0.49]	<.01
L12	Condyle (R)	x	-0.32	[-0.57,	-0.07]	.01
		y	-0.59	[-0.85,	-0.33]	<.01
		z	-0.52	[-0.87,	-0.16]	<.01
L13	Gnathion	x	-0.51	[-1.08,	0.05]	.07
		y	1.50	[0.88,	2.12]	<.01
		z	-0.88	[-1.83,	0.06]	.06
L14	Gonion (L)	x	1.70	[0.93,	2.47]	<.01
		y	-0.61	[-1.02,	-0.20]	<.01
		z	-1.05	[-1.64,	-0.47]	<.01
L15	Gonion (R)	x	-1.37	[-2.35,	-0.39]	<.01
		y	-0.76	[-1.27,	-0.24]	<.01
		z	-1.21	[-1.91,	-0.51]	<.01
L16	Md Canine (L)	x	-0.58	[-0.97,	-0.20]	<.01
		y	0.49	[0.15,	0.82]	<.01
		z	-1.81	[-2.27,	-1.34]	<.01
L17	Md Canine (R)	x	-0.57	[-0.99,	-0.15]	<.01
		y	0.44	[0.07,	0.82]	.02
		z	-1.95	[-2.46,	-1.43]	<.01
L18	Md Molar (L)§	x	-0.46	[-0.85,	-0.07]	.02
		y	0.97	[0.62,	1.31]	<.01
		z	-1.70	[-2.26,	-1.14]	<.01
L19	Md Molar (R)§	x	-0.44	[-0.84,	-0.04]	.03
		y	0.94	[0.59,	1.30]	<.01
		z	-1.92	[-2.46,	-1.37]	<.01
L20	Md Incisor (L)¥	x	-0.42	[-0.86,	0.02]	.06
		y	0.45	[0.08,	0.81]	.01
		z	-1.92	[-2.36,	-1.47]	<.01
L21	Md Incisor (L)¥	x	-0.32	[-0.78,	0.14]	.16
		y	0.42	[0.06,	0.78]	.02
		z	-1.83	[-2.28,	-1.38]	<.01
L22	Menton	x	-0.43	[-1.00,	0.13]	.12
		y	1.47	[0.88,	2.05]	<.01
		z	-0.93	[-1.89,	0.04]	.05
L23	Pogonion	x	-0.58	[-1.12,	-0.04]	.03
		y	1.56	[0.88,	2.23]	<.01
		z	-0.88	[-1.80,	0.05]	.06

Abbreviations: Mx, maxillary; Md, mandibular; L, left; R, right; CI, confidence interval.

§ First molar.

¥ Central incisor.

† Mean of the 95% confidence interval expressed in millimeters.

‡ Z critical value confidence interval. Null hypothesis was that the mean distance error was 0.

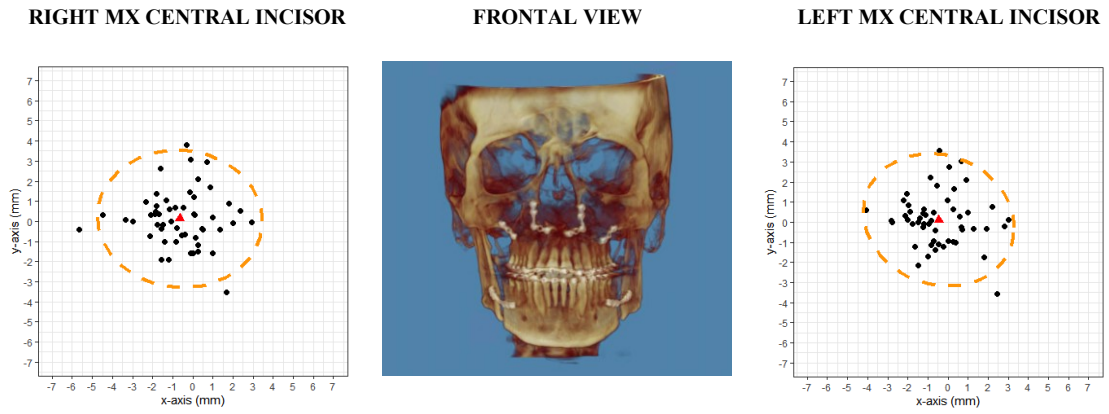

A

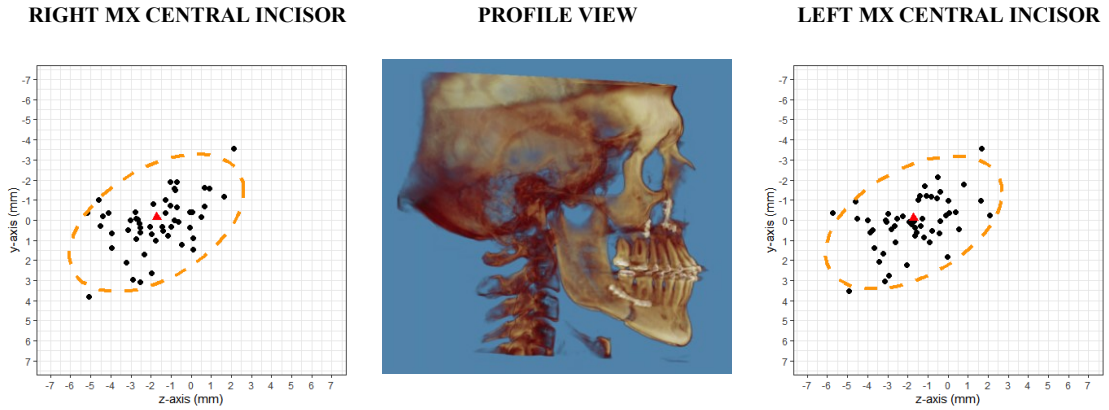

B

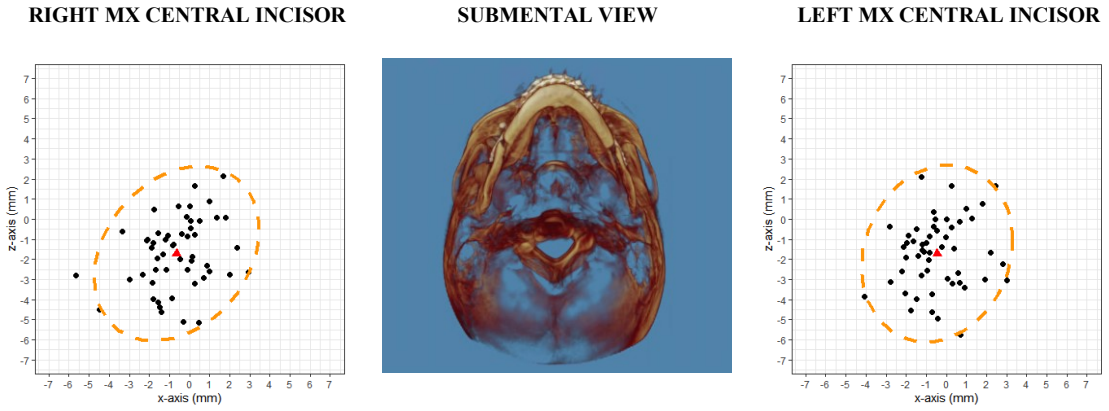

C

Figure 4. Scattergrams and 95% confidence boundary for the error for the left and right maxillary central incisors in (A) the XY plane, (B) the ZY plane, and (C) the XZ plane.

Abbreviations: MX, maxillary.

Table 6. Landmark vs mean absolute distance error (maxillary landmarks)

Landmark		Dimension	Mean (mm)†	95% CI‡	
L1	A-point	x	1.19	[1.15,	1.22]
		y	1.74	[1.68,	1.81]
		z	2.83	[2.76,	2.90]
L2	ANS	x	1.27	[1.23,	1.30]
		y	1.10	[1.06,	1.14]
		z	3.95	[3.85,	4.04]
L3	PNS	x	1.62	[1.57,	1.66]
		y	1.74	[1.69,	1.80]
		z	1.70	[1.65,	1.75]
L4	Mx Canine (L)	x	1.17	[1.14,	1.21]
		y	0.92	[0.89,	0.95]
		z	1.99	[1.93,	2.05]
L5	Mx Canine (R)	x	1.17	[1.13,	1.20]
		y	0.92	[0.89,	0.94]
		z	2.12	[2.07,	2.18]
L6	Mx Molar (L)§	x	1.33	[1.30,	1.37]
		y	1.01	[0.97,	1.04]
		z	2.15	[2.09,	2.21]
L7	Mx Molar (R)§	x	1.04	[1.01,	1.06]
		y	1.12	[1.09,	1.15]
		z	2.48	[2.42,	2.54]
L8	Mx Incisor (L)¥	x	1.26	[1.23,	1.30]
		y	0.94	[0.91,	0.98]
		z	1.98	[1.93,	2.04]
L9	Mx Incisor (R)¥	x	1.32	[1.27,	1.36]
		y	0.99	[0.96,	1.03]
		z	1.97	[1.92,	2.03]

Abbreviations: ANS, anterior nasal spine; PNS, posterior nasal spine; Mx, maxillary; Md, mandibular; L, left; R, right; CI, confidence interval.

§ First molar.

¥ Central incisor.

† Mean of the 95% confidence interval expressed in millimeters.

‡ Z critical value confidence interval.

Table 7. Landmark vs mean absolute distance error (mandibular landmarks)

Landmark		Dimension	Mean (mm)†	95% CI‡	
L10	B-point	x	1.43	[1.39,	1.48]
		y	2.14	[2.07,	2.22]
		z	2.44	[2.38,	2.51]
L11	Condyle (L)	x	0.98	[0.95,	1.01]
		y	0.69	[0.66,	0.72]
		z	0.92	[0.89,	0.95]
L12	Condyle (R)	x	0.79	[0.77,	0.81]
		y	0.80	[0.77,	0.82]
		z	1.00	[0.97,	1.04]
L13	Gnathion	x	1.59	[1.54,	1.64]
		y	1.99	[1.92,	2.05]
		z	2.75	[2.67,	2.83]
L14	Gonion (L)	x	2.17	[2.08,	2.26]
		y	1.22	[1.18,	1.26]
		z	1.79	[1.73,	1.85]
L15	Gonion (R)	x	2.47	[2.36,	2.57]
		y	1.49	[1.44,	1.54]
		z	2.27	[2.21,	2.33]
L16	Md Canine (L)	x	1.21	[1.18,	1.24]
		y	1.00	[0.97,	1.04]
		z	1.98	[1.92,	2.03]
L17	Md Canine (R)	x	1.29	[1.25,	1.32]
		y	1.07	[1.03,	1.10]
		z	2.26	[2.21,	2.32]
L18	Md Molar (L)§	x	1.16	[1.12,	1.19]
		y	1.26	[1.23,	1.30]
		z	2.12	[2.06,	2.18]
L19	Md Molar (R)§	x	1.25	[1.22,	1.28]
		y	1.24	[1.20,	1.28]
		z	2.24	[2.18,	2.30]
L20	Md Incisor (L)¥	x	1.38	[1.35,	1.41]
		y	1.06	[1.02,	1.09]
		z	2.09	[2.04,	2.14]
L21	Md Incisor (L)¥	x	1.39	[1.35,	1.42]
		y	1.05	[1.02,	1.09]
		z	2.00	[1.95,	2.06]
L22	Menton	x	1.58	[1.53,	1.63]
		y	1.87	[1.81,	1.94]
		z	2.79	[2.71,	2.88]
L23	Pogonion	x	1.58	[1.53,	1.62]
		y	2.10	[2.03,	2.18]
		z	2.69	[2.61,	2.77]

Abbreviations: Mx, maxillary; Md, mandibular; L, left; R, right; CI, confidence interval.

§ First molar.

¥ Central incisor.

† Mean of the 95% confidence interval expressed in millimeters.

‡ Z critical value confidence interval.

4.4 Maxilla-first vs Mandible-first Surgery

The *t* critical value confidence interval for the mean 3D distance error for each landmark for mandible-first surgery and maxilla-first surgery groups are presented in Table 8. The mean of the 95% confidence interval is also shown. The mean 3D distance error for all maxillary landmarks was smaller in the maxilla-first surgery group while the mean 3D distance error for all mandibular landmarks was smaller in the mandible-first surgery group except the right condyle, right mandibular canine, and gonion (left and right). Overall, the effect of surgical sequence (mandible-first or maxilla-first) on mean 3D distance error was not statistically significant.

The *t* critical value confidence interval for the mean distance error in the x, y, and z dimensions for mandible-first surgery and maxilla-first surgery groups are presented in Appendix 2, Supplemental Tables 10 and 11 for maxillary and mandibular landmarks, respectively. The mean distance error was smaller in all dimensions for all maxillary landmarks in the maxilla-first surgery group except PNS, maxillary first molar (right), and maxillary central incisor (left and right). For all maxillary landmarks in both the mandible-first and maxilla-first surgery groups, the mean distance error was largest in the z dimension (except PNS where mean distance error was largest in the y dimension for both groups).

Table 8. Landmark vs mean 3D distance error for mandible-first and maxilla-first sequence

Landmark		Mandible-first			Maxilla-first			P value*
		Mean†	95% CI‡		Mean†	95% CI‡		
L1	A-point	4.19	[3.66,	4.72]	3.22	[1.94,	4.50]	.13
L2	ANS	4.72	[4.06,	5.39]	3.93	[1.90,	5.97]	.36
L3	PNS	3.57	[3.14,	3.99]	2.57	[1.43,	3.71]	.07
L4	Mx Canine (L)	2.86	[2.40,	3.33]	2.57	[1.67,	3.47]	.55
L5	Mx Canine (R)	2.92	[2.52,	3.31]	2.60	[1.18,	4.02]	.50
L6	Mx Molar (L)§	3.18	[2.68,	3.68]	2.41	[1.68,	3.15]	.18
L7	Mx Molar (R)§	3.31	[2.95,	3.67]	2.42	[0.97,	3.87]	.08
L8	Mx Incisor (L)¥	2.91	[2.50,	3.32]	2.63	[1.48,	3.78]	.53
L9	Mx Incisor (R)¥	2.99	[2.55,	3.42]	2.68	[1.41,	3.94]	.50
L10	B-point	3.01	[2.50,	3.52]	4.16	[2.19,	6.12]	.10
L11	Condyle (L)	1.71	[1.35,	2.07]	1.79	[0.95,	2.64]	.84
L12	Condyle (R)	1.76	[1.40,	2.11]	1.35	[0.88,	1.81]	.32
L13	Gnathion	3.10	[2.53,	3.67]	4.04	[2.38,	5.70]	.21
L14	Gonion (L)	3.78	[3.05,	4.52]	2.96	[1.77,	4.16]	.46
L15	Gonion (R)	4.33	[3.40,	5.25]	3.71	[2.52,	4.90]	.63
L16	Md Canine (L)	2.76	[2.32,	3.20]	2.95	[1.65,	4.25]	.79
L17	Md Canine (R)	3.13	[2.70,	3.56]	2.87	[1.36,	4.37]	.59
L18	Md Molar (L)§	3.02	[2.58,	3.47]	3.15	[1.88,	4.42]	.83
L19	Md Molar (R)§	3.11	[2.65,	3.57]	3.19	[1.67,	4.70]	.95
L20	Md Incisor (L)¥	2.93	[2.51,	3.35]	3.16	[2.01,	4.31]	.71
L21	Md Incisor (R)¥	2.88	[2.46,	3.31]	3.15	[1.99,	4.31]	.66
L22	Menton	3.00	[2.41,	3.59]	4.16	[2.45,	5.87]	.12
L23	Pogonion	3.17	[2.58,	3.75]	4.14	[2.46,	5.83]	.20

Abbreviations: ANS, anterior nasal spine; PNS, posterior nasal spine; Mx, maxillary; Md, mandibular; L, left; R, right; CI, confidence interval.

§ First molar.

¥ Central incisor.

† Mean of the 95% confidence interval expressed in millimeters.

‡ *t* critical value confidence interval.

*ANOVA revealed no statistically significant difference between the two groups (P = .37)

Chapter 5: Discussion

5.1 Outcomes

The purpose of this study was to establish a fully digital, in-house VSP workflow for orthognathic surgery and to evaluate its accuracy. The investigators hypothesized that this workflow could provide a range of error that meets criteria for clinical acceptability commonly used in the literature.[9] The specific aim of this study was to measure the 3D distance error, as well as the mean error and mean absolute error in the left-right, superior-inferior, and anterior-posterior dimensions, for a series of landmarks between the virtual surgical plan and the actual surgical outcome.

The mean 3D distance error for the left and right maxillary central incisors was 2.86 mm and 2.93 mm, respectively. The mean distance error and mean absolute distance error for the maxillary central incisors was less than 2.0 mm in each dimension. In the literature, "2 mm" has traditionally been considered the threshold for clinical acceptability.[9] While the mean distance error and mean absolute distance error in the left-right, superior-inferior, and anterior-posterior dimensions individually met this threshold, the mean 3D distance error did not.

Based on the mean absolute error results, it was noted that the largest contributor to the 3D distance error was the anterior-posterior dimension (z axis). Additionally, the mean distance error in the anterior-posterior dimension for all landmarks was negative, indicating that there was a general tendency to under-advance (or setback) the maxillomandibular complex compared to what was planned. Others have also reported similar findings of under-advancement with occlusal splint-based surgery.[27–29] Tankersley et al. noted a significantly negative mean error of -2.0 mm at the maxillary central incisor with root mean squared deviation of 2.6 mm in the anterior-posterior dimension. While the present study found error at the maxillary incisor to be slightly less (mean error of -1.71 mm and mean absolute error of 1.97 mm), the same trends were observed. There are several factors that could potentially contribute to this finding. First, if the pre-operative CBCT is not obtained in centric relation (as was the case for this study), there is a risk of

under-advancement if using a maxilla-first surgical sequence. However, this is unlikely to be a factor in this study as 43 of 52 patients underwent mandible-first surgery and those who did undergo maxilla-first surgery experienced an under-advancement that was comparable to the mandible-first group. Another factor that could influence the degree of advancement is the intraoperative position of the condyle in the glenoid fossa. If the condyle is over-seated posteriorly in the fossa or if the condyle falls back in the fossa under general anesthesia in the supine position, there is a risk of under-advancement. Again, these examples are more relevant to a maxilla-first surgical sequence and are unlikely to be factors in this study for the reasons mentioned above. If the surgeon deviates from the planned vertical position of the maxilla, this will cause an unplanned autorotation of the maxillomandibular complex and influence the final anterior-posterior position of the landmarks. While this is possible, the error in the superior-inferior dimension in this study was found to be small, making secondary autorotation unlikely. Next, it is possible that some degree of surgical relapse occurs between the time of surgery and the time of post-operative imaging, leading to a perceived under-advancement. Finally, the under-advancement in the anterior-posterior dimension could possibly be attributed in part to a discrepancy in the planned vs actual osteotomies, however this was not specifically investigated in this study. While a clear explanation for this phenomenon was not identified, the general tendency toward deficient movement in the anterior-posterior direction (z axis) is important to consider in future case planning when using a fully digital, in-house VSP workflow for orthognathic surgery.

The mean 3D distance error was smallest for the left and right condyle which is likely related to the relatively limited movement of this landmark during surgery, although this was not tested statistically. The mean 3D distance error was largest at ANS, however this landmark is often trimmed intraoperatively. For this reason, ANS was not included in ANOVA models and its associated distance error results should be interpreted with caution. The increased error at gonion can be attributed to the increased degree of freedom in positioning the proximal mandibular segment when plating the sagittal split osteotomy. The other bony landmarks in the anterior mandible and maxilla (B-point, gnathion, menton, pogonion, and A-point) were also associated with increased mean 3D

distance error. It is possible that some of this error can be attributed to an increased difficulty in consistently labelling these landmarks due to their positions along the curvilinear symphysis and alveolus. Also, by definition, the position of these landmarks will change as the maxillomandibular complex is rotated which may contribute to the increased error.

In the mandible-first and maxilla-first surgery groups, it was found that the mean 3D distance error for maxillary landmarks was smaller in the maxilla-first surgery group, while the mean 3D distance error for mandibular landmarks except the right condyle, right mandibular canine, and gonion (left and right) was smaller in the mandible-first surgery group. It seems logical that the mean error would be smaller in the jaw that is repositioned first given that the intermediate splint is based on an uncut structure. Similarly, it is reasonable that the jaw repositioned second would have a larger mean error given that the final splint is based on a structure that has been modified by surgery. Despite this trend, the analysis of variance for the effect of surgical sequence on 3D distance error was not statistically significant.

5.2 Limitations and Areas for Improvement

Regarding the study methods, there were several limitations. Firstly, manual repeated landmark identification on the pre and postoperative digital volume is tedious and time consuming. Also noted previously, the position of some landmarks (A-point, B-point, menton, pogonion, and gnathion) will change as the maxillomandibular complex is rotated, even if by only a small amount. This makes it impossible to truly track the position of these landmarks with repeated landmark identification. To circumvent these issues, some authors have advocated for semiautomatic or automatic voxel-based analysis of surgical outcomes.[30–33] These techniques rely on regional voxel-based registration (R-VBR) of the preoperative maxillary and mandibular segments onto to their representative postoperative segments to generate a transformational matrix. The transformational matrix can then be used to calculate the displacement of any number of landmarks on the region of interest. Since the rotational and, more recently, the linear accuracy of R-VBR

has been validated for non-segmental LeFort I and bilateral sagittal split osteotomies by Han et al.[34,35], this technique should be considered for future studies involving analysis of orthognathic surgery outcomes. The second limitation with the study methods is that it is assumed the only movement that occurs between the preoperative and postoperative imaging is due to the surgery itself. However, the use of guiding elastics in the immediate postoperative period prior to imaging invariably contributes to tooth movement that is not accounted for in the study. To remove this variable, an intraoperative image would need to be acquired prior to the insertion of the final occlusal splint, which is impractical. Finally, difficulty in the recording of centric relation (which is especially important in maxilla-first surgery), replicating the planned occlusal adjustments, and reproducing the planned osteotomies all contribute to the observed distance error and are not unique to this study.[36]

There were also limitations related to the study sample. First, all patients who underwent bimaxillary orthognathic surgery were included (with some exceptions, see exclusion criteria). As a result, various surgical movements (advancement, setback, impaction etc.) were considered and therefore, the trends in surgical error that were observed in the study group may not be representative of each specific type of surgery. Similarly, the degree of surgical movement was not considered. For example, 5 of 52 patients underwent maxillomandibular advancement for obstructive sleep apnea. This patient group underwent significant advancement of the maxillomandibular complex that is non-representative of the typical bimaxillary orthognathic surgery patient and may bias the observed error. While an evaluation of the specific surgical movement and degree of movement were outside the scope of this study, considering these variables in future studies may yield results that are more applicable to specific surgical scenarios.

Relating to the sample size, 14 of 52 patients underwent concurrent genioplasty, leaving a reduced sample size of 38 patients who contributed data for the anterior mandible (see Section 3.4.5 Evaluation of the Postoperative Outcome). Additionally, only 9 patients underwent maxilla-first surgery. Therefore, findings relating to landmarks in the anterior mandible and a direct comparison of mandible-first and maxilla-first surgery landmarks may not be representative of the larger population.

5.3 Practical Considerations

While a detailed cost-benefit and feasibility analysis was beyond the scope of this study, the investigators felt it would be important to comment on the practicality of the fully digital, in-house workflow for VSP.

Apart from the obvious need to purchase new equipment, the largest barrier to implementing the workflow is likely the learning curve associated with planning software and CAD/CAM techniques. Once implemented however, the protocol is relatively straight forward. The second limitation is the additional time required to import and set-up cases, manage and troubleshoot printing equipment, as well as the processing of patient guides once printed. While these steps become more efficient with experience, they are still time consuming. At our institution, these tasks were carried out by the team of surgical residents. In a non-academic setting, they may be better suited to a skilled office technician.

In terms of the benefits to an in-house VSP workflow, there is certainly the opportunity for cost-savings. At our institution, most of the expensive equipment (CBCT and intraoral scanner) was already in place and the only additional equipment acquired was the 3D printing equipment and planning software. These upfront costs were quickly justified as the number of in-house VSP cases increased and cost per case decreased. Currently, the cost per case is a fraction of what it would be to outsource to a third party. A second benefit to the workflow is the reliability and control over case turnaround time. At our institution, a case can be prepared for surgery in one to two days if required. Finally, one of the main advantages of the fully digital, in-house VSP workflow is the opportunity to foresee the effects of the planned movements and anticipate potential complications before they arise. In our experience, it has been an invaluable tool for resident education and development.

5.4 Conclusion

A fully digital, in-house VSP workflow for orthognathic surgery was established and its accuracy evaluated. At the maxillary central incisor, the mean distance error and mean absolute distance error were within a clinically acceptable range (less than 2 mm); however, the mean 3D distance error was not. This was primarily due to deficient movement in the anterior-posterior direction (z axis). This finding was felt to be clinically valuable for treatment planning purposes when using a fully digital, in-house VSP workflow.

Appendix 1: Standardized Landmarking Protocol

Landmarks L1, L2, and L3 (A-point, ANS, and PNS) were labelled by first orienting the volume along the maxillary midline using the front and bottom views and the Mid-Sagittal Plane crosshair. The landmarks were then labelled on the volume along the maxillary midline in the Sagittal Slice view (Figure 4).

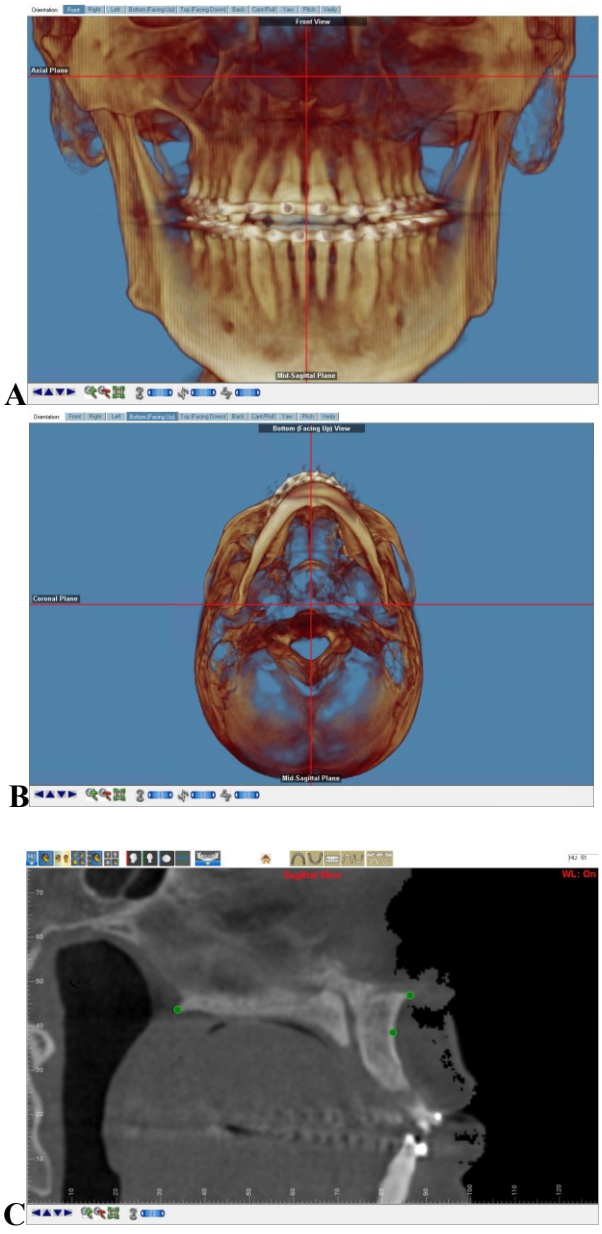

Figure 4. (A) Orienting the volume along the maxillary midline using the front and (B) bottom views and the Mid-Sagittal Plane crosshair. (C) Labelling landmarks along the maxillary midline in the Sagittal Slice view.

Landmark L9 (right maxillary incisor) was labelled by first orienting the volume along the long axis of the tooth with the Mid-Sagittal Plane crosshair. The landmark was then labelled on the volume in the Sagittal Slice view at the incisal edge (Figure 5). The same technique was used for landmarks L4, L5, L8, L16, L17, L20 and L21 (left maxillary canine, right maxillary canine, left maxillary incisor, left mandibular canine, right mandibular canine, left mandibular incisor, and right mandibular incisor).

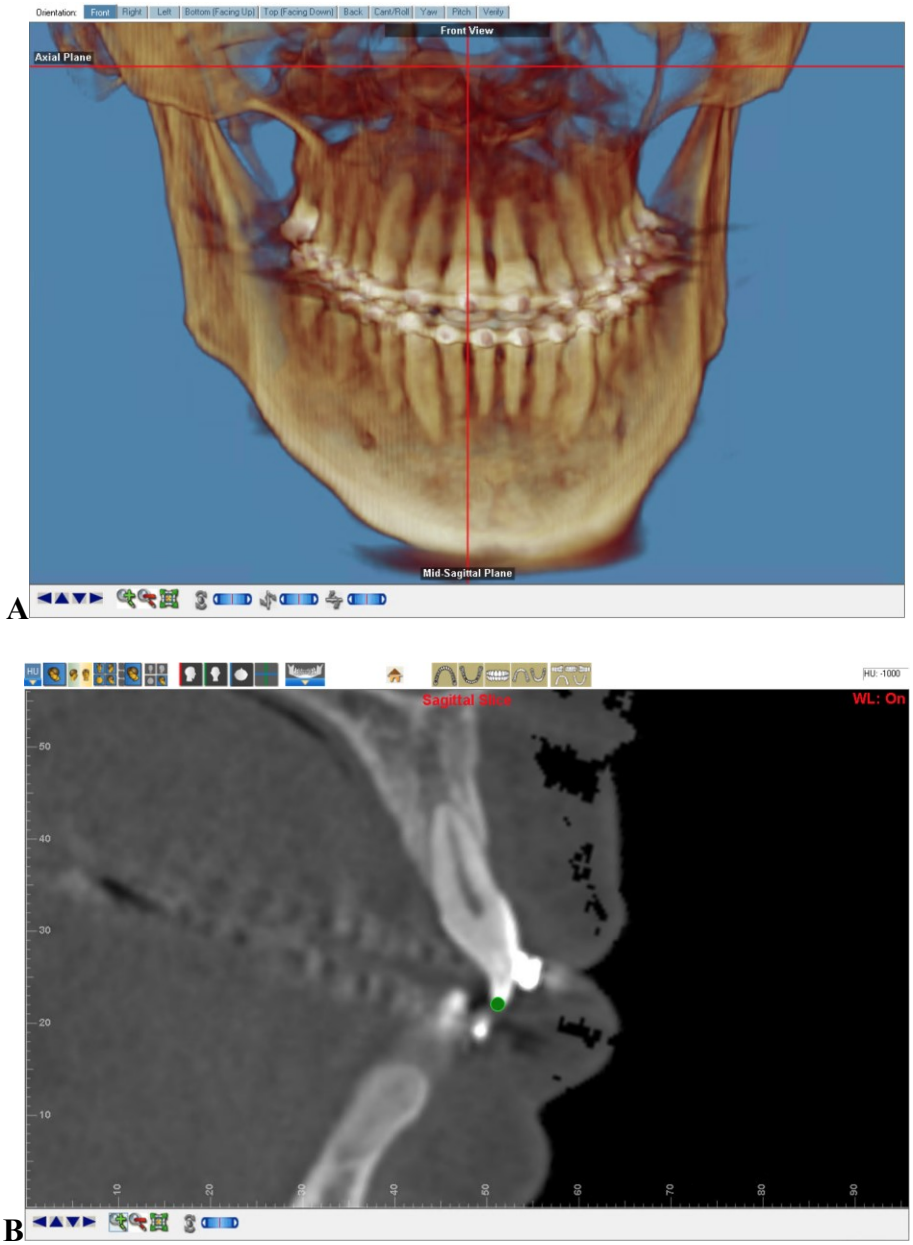

Figure 5. (A) Orienting the volume along the long axis of the maxillary central incisor with the Mid-Sagittal Plane crosshair. (B) Labelling the maxillary central incisor landmark in the Sagittal Slice view.

Landmark L7 (right maxillary molar) was labelled by first orienting the volume along the long axis of the tooth through the mesial edge of the orthodontic bracket with the Mid-Sagittal Plane crosshair. The landmark was then labelled on the volume in the Sagittal Slice view at the coronal and buccal corner of the orthodontic bracket (Figure 6). The mesial-coronal-buccal corner of the orthodontic bracket was used instead of the cusp tip because it was felt to be more reliable as the molar cusp tips are often broad and occasional modified by occlusal reduction during surgery. The same technique was used for landmarks L6, L18, and L19 (left maxillary molar, left mandibular molar, and right mandibular molar).

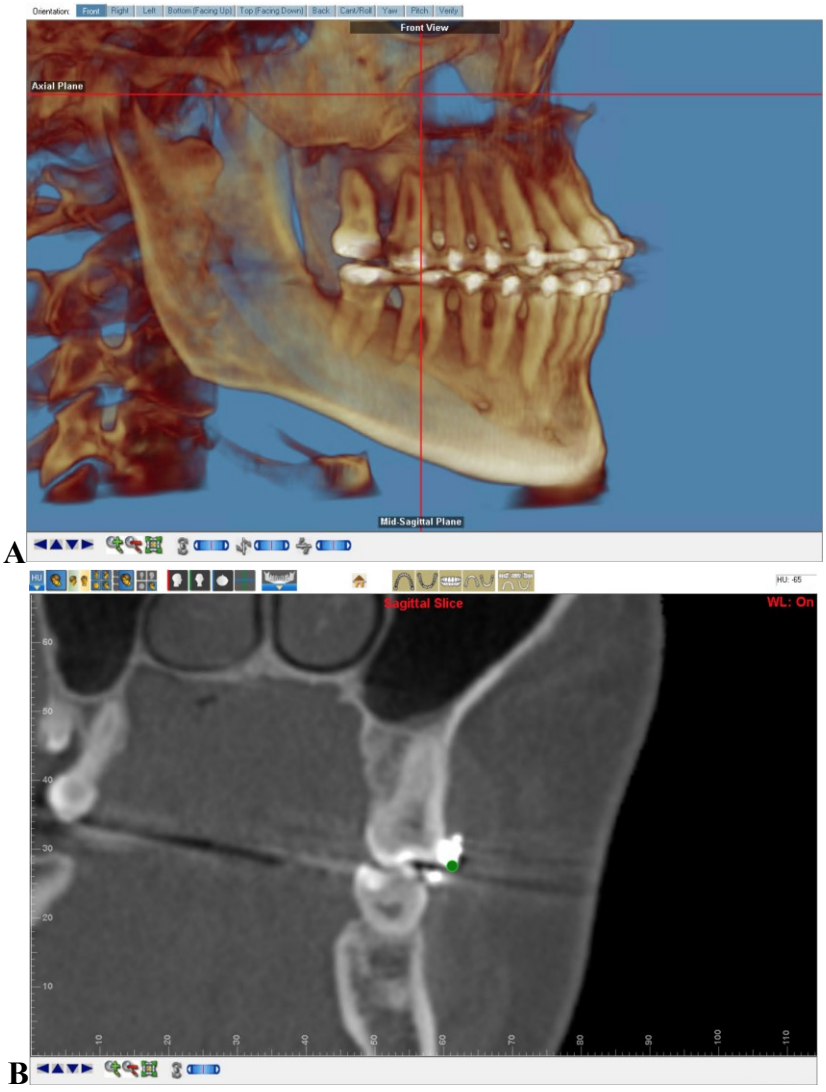

Figure 6. (A) Orienting the volume along the long axis of the maxillary first molar through the mesial edge of the orthodontic bracket. (B) Labelling the maxillary first molar landmark in the Sagittal Slice view.

Landmarks L10, L13, L22, and L23 (B-point, gnathion, menton, and pogonion) were labelled by first orienting the volume along the mandibular midline using the front and bottom views and the Mid-Sagittal Plane crosshair. The landmarks were then labelled on the volume along the mandibular midline in the Sagittal Slice view (Figure 7).

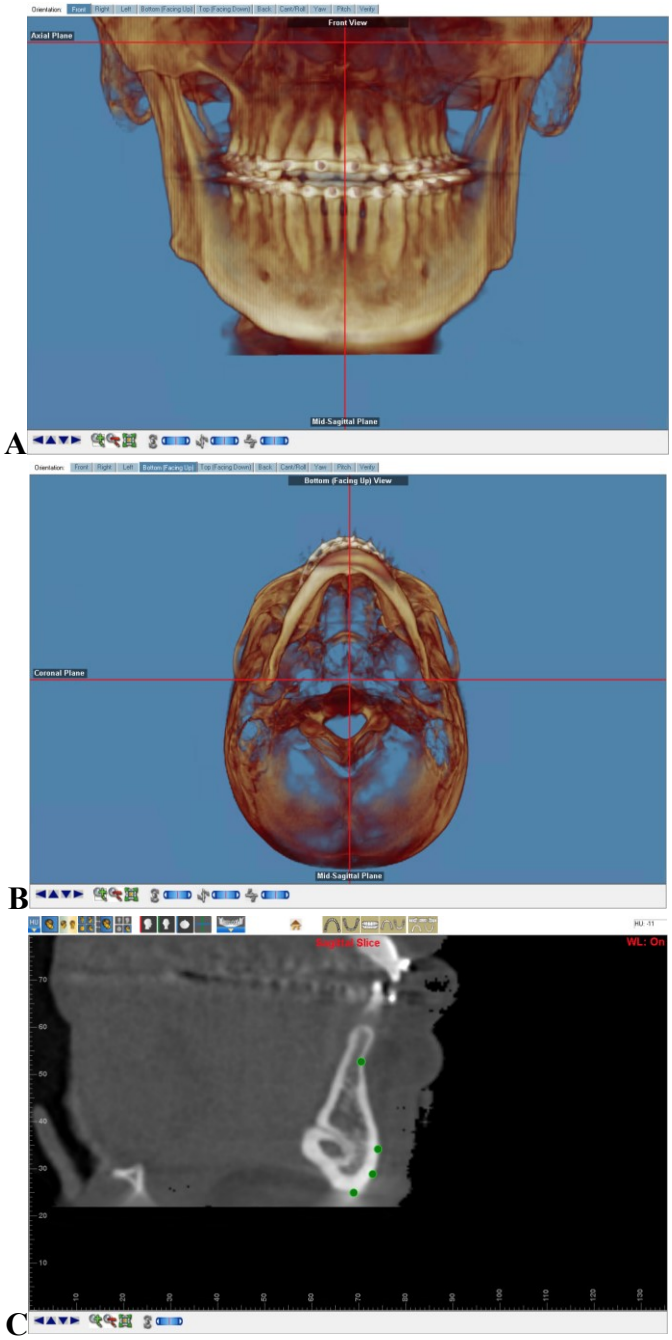

Figure 7. (A) Orienting the volume along the mandibular midline using the front and (B) bottom views and the Mid-Sagittal Plane crosshair. (C) Labelling landmarks along the mandibular midline in the Sagittal Slice view.

Landmarks L11 and L12 (left condyle and right condyle) were labelled with the volume in the mandibular midline orientation used above and by selective the widest and most cranial point on the condyle in the Coronal Slice view (Figure 8).

Figure 8. Labelling the right condyle in the Coronal Slice view.

Landmarks L14 and L15 (left gonion and right gonion) were labelled with the volume in the mandibular midline orientation used above and by selective the most inferior and posterior point at the angle of the mandible in the profile view (Figure 9).

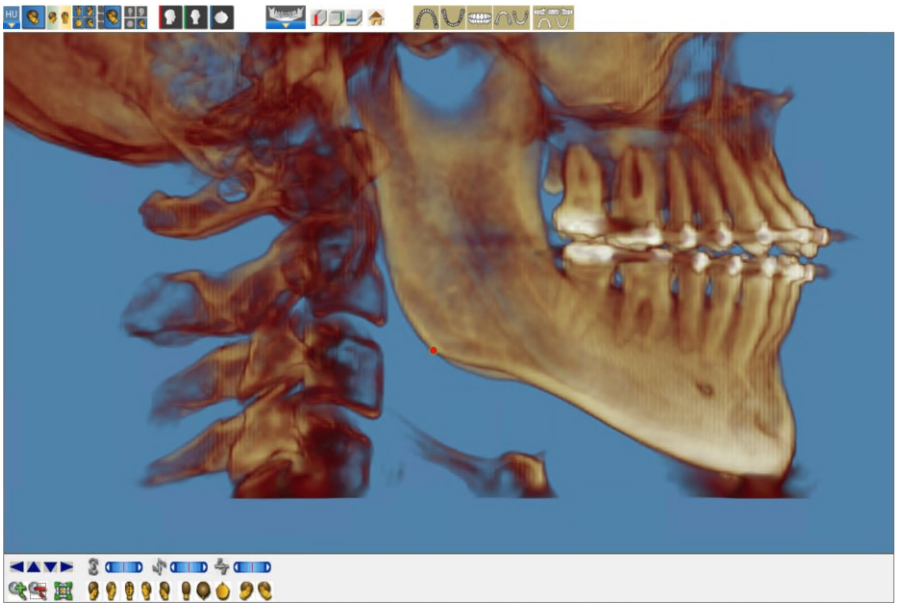

Figure 9. Labelling the right gonion in the profile view.

Appendix 2: Supplemental Data

Table 9. Sample size calculation for 3D distance error

Landmark		Sample Size	
		SE = 0.2	SE = 0.25
L1	A-point	46	29
L2	ANS	73	47
L3	PNS	46	30
L4	Mx Canine (L)	45	29
L5	Mx Canine (R)	41	26
L6	Mx Molar (L)[§]	80	51
L7	Mx Molar (R)[§]	61	39
L8	Mx Incisor (L)[¥]	37	24
L9	Mx Incisor (R)[¥]	34	22
L10	B-point	99	63
L11	Condyle (L)	34	22
L12	Condyle (R)	30	19
L13	Gnathion	133	85
L14	Gonion (L)	105	67
L15	Gonion (R)	189	121
L16	Md Canine (L)	38	25
L17	Md Canine (R)	45	29
L18	Md Molar (L)[§]	48	31
L19	Md Molar (R)[§]	57	37
L20	Md Incisor (L)[¥]	38	25
L21	Md Incisor (R)[¥]	38	24
L22	Menton	130	83
L23	Pogonion	128	82

Abbreviations: ANS, anterior nasal spine; PNS, posterior nasal spine; Mx, maxillary; Md, mandibular; L, left; R, right; SE, standard error.

[§] First molar.

[¥] Central incisor.

Table 10. Mean distance error for mandible-first and maxilla-first surgery (maxillary landmarks)

	Landmark	Dimension	Mandible-first Surgery				Maxilla-first Surgery			
			Mean[†]	95% CI[‡]		*P* value	Mean[†]	95% CI[‡]		*P* value
L1	A-point	x	-0.73	[-1.14,	-0.31]	<.01	-0.16	[-1.39,	1.08]	.78
		y	-1.05	[-1.70,	-0.40]	<.01	-0.68	[-2.66,	1.31]	.46
		z	-3.04	[-3.63,	-2.45]	<.01	-1.22	[-2.55,	0.11]	.07
L2	ANS	x	-0.77	[-1.20,	-0.34]	<.01	-0.06	[-1.33,	1.20]	.91
		y	-0.15	[-0.62,	0.31]	.51	-0.04	[-1.13,	1.06]	.94
		z	-4.04	[-4.79,	-3.29]	<.01	-3.35	[-5.39,	-1.32]	<.01
L3	PNS	x	-0.44	[-1.09,	0.20]	.17	-0.46	[-1.60,	0.68]	.38
		y	1.35	[0.78,	1.91]	<.01	0.84	[-0.81,	2.49]	.27
		z	-1.20	[-1.79,	-0.62]	<.01	-0.62	[-1.52,	0.29]	.16
L4	Mx Canine (L)	x	-0.71	[-1.10,	-0.33]	<.01	-0.26	[-1.73,	1.21]	.69
		y	0.46	[0.08,	0.83]	.02	0.33	[-0.43,	1.09]	.34
		z	-1.90	[-2.45,	-1.35]	<.01	-1.17	[-2.36,	0.02]	.05
L5	Mx Canine (R)	x	-0.44	[-0.83,	-0.04]	.03	-0.33	[-1.81,	1.14]	.62
		y	0.55	[0.21,	0.89]	<.01	0.43	[-0.27,	1.13]	.2
		z	-1.91	[-2.46,	-1.35]	<.01	-1.37	[-2.92,	0.18]	.08
L6	Mx Molar (L)[§]	x	-0.95	[-1.36,	-0.54]	<.01	-0.42	[-1.71,	0.86]	.47
		y	0.72	[0.35,	1.10]	<.01	0.12	[-0.78,	1.02]	.76
		z	-1.99	[-2.62,	-1.35]	<.01	-1.26	[-2.13,	-0.39]	.01
L7	Mx Molar (R)[§]	x	-0.20	[-0.57,	0.18]	.29	-0.50	[-1.58,	0.57]	.31
		y	0.88	[0.53,	1.23]	<.01	0.12	[-0.62,	0.86]	.72
		z	-2.32	[-2.90,	-1.74]	<.01	-1.34	[-3.05,	0.37]	.11
L8	Mx Incisor (L)[¥]	x	-0.51	[-0.94,	-0.09]	.02	-0.15	[-1.68,	1.38]	.83
		y	0.08	[-0.33,	0.50]	.69	0.28	[-0.56,	1.11]	.47
		z	-1.79	[-2.33,	-1.24]	<.01	-1.33	[-2.61,	-0.06]	.04
L9	Mx Incisor (R)[¥]	x	-0.70	[-1.17,	-0.22]	<.01	-0.37	[-1.94,	1.20]	.6
		y	0.10	[-0.34,	0.54]	.64	0.27	[-0.56,	1.09]	.48
		z	-1.81	[-2.33,	-1.28]	<.01	-1.28	[-2.69,	0.13]	.07

Abbreviations: ANS, anterior nasal spine; PNS, posterior nasal spine; Mx, maxillary; Md, mandibular; L, left; R, right; CI, confidence interval.

[§] First molar.

[¥] Central incisor.

[†] Mean of the 95% confidence interval expressed in millimeters.

[‡] *t* critical value confidence interval. Null hypothesis was that the mean distance error was 0 for each dimension of each landmark.

Table 11. Mean distance error for mandible-first and maxilla-first surgery (mandibular landmarks)

	Landmark	Dimension	Mandible-first Surgery			Maxilla-first Surgery			
			Mean†	95% CI‡	*P* value	Mean†	95% CI‡	*P* value	
L10	B-point	x	-0.50	[-1.04, 0.05]	0.07	-0.66	[-1.97, 0.65]	.28	
		y	1.60	[0.87, 2.33]	<.01	0.74	[-1.70, 3.19]	.5	
		z	-1.13	[-1.99, -0.28]	.01	-1.96	[-4.06, 0.15]	.07	
L11	Condyle (L)	x	0.19	[-0.18, 0.56]	.31	0.76	[-0.33, 1.86]	.15	
		y	-0.52	[-0.81, -0.23]	<.01	-0.58	[-1.05, -0.10]	.02	
		z	-0.77	[-1.10, -0.45]	<.01	-0.76	[-1.42, -0.10]	.03	
L12	Condyle (R)	x	-0.36	[-0.65, -0.07]	.02	-0.15	[-0.65, 0.36]	.52	
		y	-0.53	[-0.83, -0.23]	<.01	-0.86	[-1.38, -0.35]	<.01	
		z	-0.54	[-0.96, -0.12]	.01	-0.40	[-0.93, 0.14]	.13	
L13	Gnathion	x	-0.40	[-1.02, 0.21]	.19	-1.04	[-2.66, 0.58]	.18	
		y	1.64	[0.95, 2.33]	<.01	0.82	[-0.91, 2.56]	.31	
		z	-0.71	[-1.67, 0.26]	.15	-1.72	[-5.20, 1.76]	.29	
L14	Gonion (L)	x	1.79	[0.89, 2.69]	<.01	1.27	[-0.28, 2.82]	.09	
		y	-0.59	[-1.04, -0.14]	.01	-0.70	[-1.93, 0.53]	.23	
		z	-1.15	[-1.82, -0.48]	<.01	-0.59	[-1.90, 0.72]	.33	
L15	Gonion (R)	x	-1.40	[-2.55, -0.24]	.02	-1.23	[-2.87, 0.41]	.12	
		y	-0.72	[-1.28, -0.16]	.01	-0.93	[-2.57, 0.72]	.23	
		z	-1.16	[-1.97, -0.35]	<.01	-1.42	[-2.92, 0.08]	.06	
L16	Md Canine (L)	x	-0.59	[-1.00, -0.19]	<.01	-0.53	[-1.92, 0.87]	.41	
		y	0.53	[0.14, 0.93]	<.01	0.27	[-0.40, 0.94]	.38	
		z	-1.78	[-2.27, -1.29]	<.01	-1.93	[-3.47, -0.38]	.02	
L17	Md Canine (R)	x	-0.61	[-1.08, -0.15]	.01	-0.35	[-1.54, 0.84]	.52	
		y	0.52	[0.08, 0.96]	.02	0.06	[-0.63, 0.76]	.84	
		z	-1.99	[-2.51, -1.46]	<.01	-1.77	[-3.68, 0.14]	.07	
L18	Md Molar (L)§	x	-0.43	[-0.85, -0.02]	.04	-0.57	[-1.85, 0.72]	.34	
		y	1.01	[0.62, 1.40]	<.01	0.78	[-0.09, 1.65]	.07	
		z	-1.63	[-2.25, -1.00]	<.01	-2.07	[-3.60, -0.55]	.01	
L19	Md Molar (R)§	x	-0.42	[-0.87, 0.03]	.07	-0.52	[-1.61, 0.57]	.31	
		y	1.04	[0.63, 1.45]	<.01	0.48	[-0.23, 1.19]	.16	
		z	-1.90	[-2.46, -1.35]	<.01	-1.97	[-4.08, 0.14]	.06	

Table 11 continued. Mean distance error for mandible-first and maxilla-first surgery (mandibular landmarks)

L20	Md Incisor (L)[¥]	x	-0.52	[-0.98,	-0.05]	.03	0.06	[-1.40,	1.53]	.92
		y	0.50	[0.08,	0.92]	.02	0.19	[-0.57,	0.96]	.58
		z	-1.91	[-2.37,	-1.44]	<.01	-1.96	[-3.59,	-0.33]	.02
L21	Md Incisor (L)[¥]	x	-0.41	[-0.90,	0.07]	.09	0.12	[-1.42,	1.66]	.86
		y	0.48	[0.07,	0.89]	.02	0.15	[-0.68,	0.98]	.68
		z	-1.84	[-2.30,	-1.37]	<.01	-1.77	[-3.44,	-0.11]	.04
L22	Menton	x	-0.33	[-0.95,	0.30]	.30	-0.95	[-2.54,	0.64]	.2
		y	1.55	[0.90,	2.20]	<.01	1.06	[-0.53,	2.64]	.16
		z	-0.73	[-1.71,	0.26]	.14	-1.88	[-5.46,	1.71]	.26
L23	Pogonion	x	-0.48	-1.07	0.11]	.11	-1.02	[-2.60,	0.56]	.18
		y	1.78	1.05	2.50]	<.01	0.49	[-1.48,	2.46]	.58
		z	-0.68	-1.62	0.25]	.15	-1.81	[-5.27,	1.65]	.26

Abbreviations: Mx, maxillary; Md, mandibular; L, left; R, right; CI, confidence interval.

[§] First molar.

[¥] Central incisor.

[†] Mean of the 95% confidence interval expressed in millimeters.

[‡] *t* critical value confidence interval. Null hypothesis was that the mean distance error was 0 for each dimension of each landmark

Bibliography

1. Gateno J, Xia JJ, Teichgraeber JF, et al. Clinical Feasibility of Computer-Aided Surgical Simulation (CASS) in the Treatment of Complex Cranio-Maxillofacial Deformities. J Oral Maxillofac Surg 2007;65(4):728–34.
2. Swennen GRJ, Mollemans W, Schutyser F. Three-Dimensional Treatment Planning of Orthognathic Surgery in the Era of Virtual Imaging. J Oral Maxillofac Surg 2009;67(10):2080–92.
3. de Waard O, Baan F, Verhamme L, Breuning H, Kuijpers-Jagtman AM, Maal T. A novel method for fusion of intra-oral scans and cone-beam computed tomography scans for orthognathic surgery planning. J Cranio-Maxillofac Surg 2016;44(2):160–6.
4. Ho CT, Lin HH, Lo LJ. Intraoral Scanning and Setting up the Digital Final Occlusion in Three-Dimensional Planning of Orthognathic Surgery: Its Comparison with the Dental Model Approach. Plast Reconstr Surg 2019;143(5):1027e–36e.
5. Beek DM, Baan F, Liebregts J, Bergé S, Maal T, Xi T. Surgical accuracy in 3D planned bimaxillary osteotomies: intraoral scans and plaster casts as digital dentition models. Int J Oral Maxillofac Surg 2022;51(7):922–8.
6. Ritto FG, Schmitt ARM, Pimentel T, Canellas J V., Medeiros PJ. Comparison of the accuracy of maxillary position between conventional model surgery and virtual surgical planning. Int J Oral Maxillofac Surg 2018;47(2):160–6.
7. Hanafy M, Akoush Y, Abou-ElFetouh A, Mounir RM. Precision of orthognathic digital plan transfer using patient-specific cutting guides and osteosynthesis versus mixed analogue–digitally planned surgery: a randomized controlled clinical trial. Int J Oral Maxillofac Surg 2020;49(1):62–8.
8. Chen Z, Mo S, Fan X, You Y, Ye G, Zhou N. A Meta-analysis and Systematic Review Comparing the Effectiveness of Traditional and Virtual Surgical Planning for Orthognathic Surgery: Based on Randomized Clinical Trials. J Oral Maxillofac Surg 2021;79(2):471.e1-471.e19.
9. Stokbro K, Aagaard E, Torkov P, Bell RB, Thygesen T. Virtual planning in orthognathic surgery. Int J Oral Maxillofac Surg 2014;43(8):957–65.
10. Schneider D, Kämmerer PW, Hennig M, Schön G, Thiem DGE, Bschorer R. Customized virtual surgical planning in bimaxillary orthognathic surgery: a prospective randomized trial. Clin Oral Investig 2019;23(7):3115–22.
11. Chen H, Jiang N, Bi R, et al. Comparison of the Accuracy of Maxillary Repositioning Between Using Splints and Templates in 2-Jaw Orthognathic Surgery. J Oral Maxillofac Surg 2022;80(8):1331–9.
12. Karanxha L, Rossi D, Hamanaka R, et al. Accuracy of splint vs splintless technique for virtually planned orthognathic surgery: A voxel-based three-dimensional analysis. J Cranio-Maxillofac Surg 2021;49(1):1–8.
13. Li B, Shen S, Jiang W, et al. A new approach of splint-less orthognathic surgery using a personalized orthognathic surgical guide system: A preliminary study. Int J Oral Maxillofac Surg 2017;46(10):1298–305.

14. Heufelder M, Wilde F, Pietzka S, et al. Clinical accuracy of waferless maxillary positioning using customized surgical guides and patient specific osteosynthesis in bimaxillary orthognathic surgery. J Cranio-Maxillofac Surg 2017;45(9):1578–85.
15. Stokbro K, Bell RB, Thygesen T. Patient-Specific Printed Plates Improve Surgical Accuracy In Vitro. J Oral Maxillofac Surg 2018;76(12):2647.e1-2647.e9.
16. Mazzoni S, Bianchi A, Schiariti G, Badiali G, Marchetti C. Computer-Aided Design and Computer-Aided Manufacturing Cutting Guides and Customized Titanium Plates Are Useful in Upper Maxilla Waferless Repositioning. J Oral Maxillofac Surg 2015;73(4):701–7.
17. Jones JP, Amarista FJ, Jeske NA, Szalay D, Ellis E. Comparison of the Accuracy of Maxillary Positioning With Interim Splints Versus Patient-Specific Guides and Plates in Executing a Virtual Bimaxillary Surgical Plan. J Oral Maxillofac Surg W.B. Saunders; 2022. p. 827–37.
18. Kraeima J, Schepers RH, Spijkervet FKL, et al. Splintless surgery using patient-specific osteosynthesis in Le Fort I osteotomies: a randomized controlled multi-centre trial. Int J Oral Maxillofac Surg 2020;49(4):454–60.
19. Mendez BM, Chiodo M V., Patel PA. Customized "in-office" three-dimensional printing for virtual surgical planning in craniofacial surgery. J Craniofac Surg 2015;26(5):1584–6.
20. Abo Sharkh H, Makhoul N. In-House Surgeon-Led Virtual Surgical Planning for Maxillofacial Reconstruction. J Oral Maxillofac Surg 2020;78(4):651–60.
21. Mascarenhas W, Makhoul N. Efficient in-house 3D printing of an orthognathic splint for single-jaw cases. Int J Oral Maxillofac Surg 2021;50(8):1075–7.
22. De Riu G, Vaira LA, Ligas E, et al. New protocol for in-house management of computer assisted orthognathic surgery. Br J Oral Maxillofac Surg 2020;58(10):e265–71.
23. Cassi D, De Biase C, Tonni I, Gandolfini M, Di Blasio A, Piancino MG. Natural position of the head: review of two-dimensional and three-dimensional methods of recording. Br J Oral Maxillofac Surg 2016;54(3):233–40.
24. Delaire J, Schendel SA, Tulasne JF. An architectural and structural craniofacial analysis: A new lateral cephalometric analysis. Oral Surg, Oral Med, Oral Path 1981;52(3):226–38.
25. Gaber RM, Shaheen E, Falter B, et al. A Systematic Review to Uncover a Universal Protocol for Accuracy Assessment of 3-Dimensional Virtually Planned Orthognathic Surgery. J Oral Maxillofac Surg 2017;75(11):2430–40.
26. Andriola F de O, Haas Junior OL, Guijarro-Martínez R, et al. Computed tomography imaging superimposition protocols to assess outcomes in orthognathic surgery: a systematic review with comprehensive recommendations. Dentomaxillofac Radiol
27. Tankersley AC, Nimmich MC, Battan A, Griggs JA, Caloss R. Comparison of the Planned Versus Actual Jaw Movement Using Splint-Based Virtual Surgical Planning: How Close Are We at Achieving the Planned Outcomes? J Oral Maxillofac Surg 2019;77(8):1675–80.
28. Chin SJ, Wilde F, Neuhaus M, Schramm A, Gellrich NC, Rana M. Accuracy of virtual surgical planning of orthognathic surgery with aid of CAD/CAM fabricated surgical splint—A novel 3D analyzing algorithm. J Cranio-Maxillofac Surg 2017;45(12):1962–70.

29. De Riu G, Virdis PI, Meloni SM, Lumbau A, Vaira LA. Accuracy of computer-assisted orthognathic surgery. J Cranio-Maxillofac Surg 2018;46(2):293–8.
30. Xi T, van Luijn R, Baan F, et al. Landmark-Based Versus Voxel-Based 3-Dimensional Quantitative Analysis of Bimaxillary Osteotomies: A Comparative Study. J Oral Maxillofac Surg 2020;78(3):468.e1-468.e10.
31. Holte MB, Diaconu A, Ingerslev J, Thorn JJ, Pinholt EM. Virtual Analysis of Segmental Bimaxillary Surgery: A Validation Study. J Oral Maxillofac Surg 2021;79(11):2320–33.
32. Baan F, Liebregts J, Xi T, et al. A new 3D tool for assessing the accuracy of bimaxillary surgery: The OrthoGnathicanAlyser. PLoS One 2016;11(2).
33. Stokbro K, Thygesen T. A 3-Dimensional Approach for Analysis in Orthognathic Surgery—Using Free Software for Voxel-Based Alignment and Semiautomatic Measurement. J Oral Maxillofac Surg 2018;76(6):1316–26.
34. Han DMD, Graca S, Kwon TG, Borba AM, Antonini F, Miloro M. What Do We Know Beyond Reliability in Voxel-Based Registration? Validation of the Accuracy of Regional Voxel-Based Registration (R-VBR) Techniques for Orthognathic Surgery Analysis. J Oral Maxillofac Surg 2022;80(2):296–302.
35. Han MD, Kwon TG, Miloro M, Chakrabarty S. What Is the Linear Accuracy of Regional Voxel-Based Registration for Orthognathic Surgery Landmarks? J Oral Maxillofac Surg 2023;81(5):546–56.
36. Caminiti M, Han MD. Digital Data Acquisition and Treatment Planning in Orthognathic Surgery. In: Miloro M, Ghali GE, Larsen PE, Waite P, editors. Peterson's Principles of Oral and Maxillofacial Surgery. Springer; 2022. p. 1767–99.